Материаловедение / Material science

УДК 620.186:620.178.74:539.42
DOI 10.17073/0368-0797-2023-3-311-319

Оригинальная статья
Original article

Влияние ускоренного охлаждения после поперечно-винтовой прокатки на формирование структуры и низкотемпературную вязкость разрушения низкоуглеродистой стали

А. И. Гордиенко, И. В. Власов, Ю. И. Почивалов

Институт физики прочности и материаловедения Сибирского отделения РАН (Россия, 634055, Томск, пр. Академический 2/4)

mirantil@ispms.ru

Аннотация. Исследуется влияние ускоренного охлаждения после поперечно-винтовой прокатки низкоуглеродистой стали класса прочности К60 на формирование структуры и механические свойства при статическом растяжении и ударном изгибе. Показано, что использование прерванного ускоренного охлаждения стали после прокатки с выдержкой при 530 °С (режим *I*) и непрерывного ускоренного охлаждения (режим *II*) приводит к формированию разного типа и соотношения количества структур в стали. После прокатки по режиму *I* структура характеризуется присутствием феррита, троостита, гранулярного бейнита и мелкодисперсных карбидов Fe_3C. После прокатки по режиму *II* структура отличается наличием реечного бейнита и крупных участков мартенситно-аустенитной (МА) составляющей размерами до 1 – 2 мкм. Уменьшение дисперсности ферритных зерен в стали после прокатки по режимам *I* и *II* с 12 до 4,6 – 4,3 мкм, формирование бейнитной фазы и упрочнение матрицы карбидами приводит к повышению пределов текучести стали до 440 и 490 МПа и пределов прочности до 760 и 880 МПа. Проведение поперечно-винтовой прокатки по режиму *I* позволяет существенно увеличить низкотемпературную вязкость разрушения стали (160 Дж/см^2) по сравнению с горячекатаным состоянием (11 Дж/см^2) и снизить хладноломкость стали в область температур ниже –50 °С. Применение непрерывного ускоренного охлаждения (режим *II*) не позволяет повысить хладостойкость стали вследствие формирования структуры реечного бейнита и крупных областей МА составляющей.

Ключевые слова: низкоуглеродистая сталь, поперечно-винтовая прокатка, ускоренное охлаждение, микроструктура, прочность, вязкость разрушения

Благодарности: Работа выполнена в рамках государственного задания Института физики прочности и материаловедения Сибирского отделения РАН, проект FWRW- 2021-0009.
Авторы благодарят И.П. Мишина и Е.Е. Найденкина за содействие в проведении поперечно-винтовой прокатки стали.
Микроструктурные исследования проведены с помощью оборудования ЦКП «Нанотех» Института физики прочности и материаловедения Сибирского отделения РАН (Centre “Nanotech” of the ISPMS SB RAS).

Для цитирования: Гордиенко А.И., Власов И.В., Почивалов Ю.И. Влияние ускоренного охлаждения после поперечно-винтовой прокатки на формирование структуры и низкотемпературную вязкость разрушения низкоуглеродистой стали. *Известия вузов. Черная металлургия*. 2023;66(3):311–319. https://doi.org/10.17073/0368-0797-2023-3-311-319

Effect of accelerated cooling after cross-helical rolling on formation of structure and low-temperature fracture toughness of low-carbon steel

A. I. Gordienko, I. V. Vlasov, Yu. I. Pochivalov

Institute of Strength Physics and Materials Science, Siberian Branch of the Russian Academy of Sciences (2/4 Akademicheskii Ave., Tomsk 634055, Russian Federation)

mirantil@ispms.ru

Abstract. The effect of accelerated cooling after cross-helical rolling of X70 low-carbon steel on the formation of structures and mechanical properties under static tension and impact bending was investigated. The use of interrupted accelerated cooling of steel after cross-helical rolling with exposure at 530 °C (mode *I*) and continuous accelerated cooling (mode *II*) leads to the formation of different types and ratios of structures in steel. After

rolling according to mode *I*, the structure is characterized by the presence of ferrite, troostite, granular bainite, and fine Fe_3C carbides. After rolling according to mode *II*, the structure is characterized by the formation of lath bainite and large sections of the martensitic-austenitic (MA) component up to 1 – 2 μm in size. It is shown that a decrease in the fineness of ferrite grains in steel after cross-helical rolling in modes *I* and *II* from 12 to 4.6 – 4.3 μm, the formation of a bainitic phase, and hardening of the matrix with carbides led to an increase in the yield strength of steel up to 440 and 490 MPa and tensile strength up to 760 and 880 MPa. Carrying out helical rolling according to mode *I* makes it possible to significantly increase the low-temperature fracture toughness of steel ($KCV^{-70\,°C}$ = 160 J/cm^2) compared to the hot-rolled state ($KCV^{-70\,°C}$ = 11 J/cm^2) and reduce the cold brittleness of steel to the temperatures below –50 °C. The use of continuous accelerated cooling (mode *II*) does not allow increasing the cold resistance of steel due to the formation of the lath bainite structure and large areas of the MA component.

Keywords: low-carbon steel, cross-helical rolling, accelerated cooling, microstructure, strength, fracture toughness

Acknowledgements: The work was performed within the framework of the state task of the Institute of Strength Physics and Materials Science, Siberian Branch of Russian Academy of Sciences, project FWRW- 2021-0009.
The authors express their gratitude to Mishin I.P. and Naydenkin E.E. for their assistance in carrying out steel cross-helical rolling.
Microstructural studies were carried out using the equipment of the Centre "Nanotech" of the Institute of Strength Physics and Materials Science, Siberian Branch of Russian Academy of Sciences.

For citation: Gordienko A.I., Vlasov I.V., Pochivalov Yu.I. Effect of accelerated cooling after cross-helical rolling on formation of structure and low-temperature fracture toughness of low-carbon steel. *Izvestiya. Ferrous Metallurgy*. 2023;66(3):311–319.
https://doi.org/10.17073/0368-0797-2023-3-311-319

Introduction

Low-carbon low alloy steels are extensively utilized in various industries. The enhancement of mechanical properties of steels is accomplished through integrated micro-doping and different modes of thermomechanical processing [1 – 11]. However, the improvement in strength is often accompanied by a decrease in plastic properties and fracture toughness, particularly under low temperatures [1; 2]. Thus, the primary objective is to increase the low-temperature fracture toughness of such steels. Factors that contribute to its increase include grain refinement [3 – 6], reduction in the fraction and grain size of pearlite [5; 6] and the martensite-austenite (MA) constituent [7]. Additionally, a more uniform alternation of ferrite and pearlite [5; 8; 9], as well as the absence of a predominant orientation of planes {001} [3], promote increased fracture toughness. Another factor that improves the cold resistance of steel is the utilization of accelerated cooling (with cooling rates V_{cool}, ranging from 5 to 30 °C/s) after rolling, leading to the formation of ferrite-bainite structures. Depending on the temperature range of rolling, start and finish temperatures of accelerated cooling, cooling rates, and holding time, different types of bainite structures can be formed, achieving varying levels of strength and fracture toughness [8 – 10]. In most studies [2 – 4; 7 – 10], the structure and mechanical properties of steels were examined after conventional longitudinal rolling. In contrast to the longitudinal process, cross-helical rolling involves a rotating reciprocal motion of ingots, resulting in a higher fraction of shift deformation component. This facilitates more efficient refinement of the granular structure in a lower number of passes, promoting the formation of a homogeneous structure and simultaneous increase in strength and low-temperature fracture toughness [5; 6; 11].

The objective of this study is to analyze the impact of accelerated cooling following cross-helical rolling of low-carbon X70 steel on the formation of its structure. Additionally, the investigation aims to examine the mechanical properties and micromechanisms of steel fracture under static tension and impact bending conditions.

Experimental

The study focused on low-carbon low alloy steel, specifically grade X70, which was in the state after hot rolling. The chemical composition of the steel (wt. %) was as follows: C 0.13; Mn 1.6; V 0.05; Nb 0.04; Si 0.4; Ti 0.05; Cu 0.3; Al 0.03; P 0.013; S 0.01. The ingots used for cross-helical rolling were obtained by cutting a hot-rolled steel sheet with a thickness of 56 mm. The initial diameter of the ingot before rolling was 40 mm. Cross-helical rolling was conducted using an RSP 14-40 three roll mill in six passes, gradually reducing the diameter. Previous research [11] demonstrated that rolling this steel at 850 °C in the region where (γ + α) phases exist in the phase diagram, following by air cooling, resulted in higher fracture toughness compared to rolling at 1000, 920 and 810 °C. In this study, the rolling process was performed at 850 °C. After rolling, accelerated cooling was applied using a water sprayer at a rate of 6 °C/s until reaching 530 °C, followed by a three-minute hold and subsequent cooling at a rate of 6 °C/s to 200 °C (mode *I*). In the second case, the ingot was cooled at a rate of 6 °C/s to 200 °C (mode *II*). Cumulative degree of deformation $\varepsilon = \ln\left(\frac{S_0}{S_f}\right)$ (where S_0 and S_f represent the initial and final surface areas of the transversal cross sections of the rods), after six rolling passes in both cases, was approximately 1.6. The final diameter of the rods after rolling was 17 mm.

Microstructural studies were conducted using a scanning electron microscope (LEO EVO 50). To prepare the samples for structural analysis, their surfaces were sequentially polished using emery paper with gradually decreasing abrasive grain sizes. Subsequently, the samples were polished on cloth using diamond paste.

In order to reveal grain boundaries, the polished surfaces were etched in a 3 % alcohol solution of HNO_3. Vickers microhardness measurements were performed using a PMT-3 hardness meter with a load of 0.49 N. For static tension tests, samples with a working area size of 15×3×1 mm were used. Impact tests were carried out on samples with dimensions of 10×10×55 mm, which featured a *V*-notch. An INSTRON MPX 450 impact machine was used for these tests within a temperature range T_{test} from +20 to –70 °C. By measuring the surface areas under the load-deflection curves, the work of crack nucleation (the surface area under the loading curve until reaching the maximum load F_{max}) and crack propagation (the surface area under the loading curve after reaching F_{max}) were determined. The stages of crack propagation and the micromechanisms of fracture at each stage were analyzed by examining the surfaces of the fractured samples using a scanning electron microscope (LEO EVO 50). The fracture surfaces were examined to identify regions exhibiting brittle fracture and shear lips. Shear lips refer to segments of ductile fracture adjacent to the lateral sides of the sample and are typically oriented at an angle of approximately 45° to them. The fractions of these regions were calculated as the ratio of their surface areas to the surface area of the cross section of the sample under the notch after fracture. The temperature of the viscous brittle transition, T_{50} (or $FATT_{50}$ [12]), was determined based on the fraction of the brittle region observed on the fracture surface. T_{50} corresponded to the temperature at which 50 % of the fracture surface exhibited brittle fracture.

Results

In the hot rolled state, X70 steel exhibits a ferrite-sorbite structure (Fig. 1, *a*). The average size (d_F) of ferrite grains is 12 μm. The volumetric fraction of sorbite (dispersed pearlite) is 20 %, and the interplanar distance in sorbite is 0.25 μm. The microhardness of the ferrite regions is measured at 165 HV_{50}.

After cross-helical rolling of the steel, the structure becomes refined and shows a more homogeneous distribution of structural constituents (Fig. 1, *b*, *d*). In the case of processing according to mode *I*, the cooling rate is insufficient to suppress diffusion decomposition of austenite. As a result, additional holding during cooling creates conditions for carbon diffusion.

In the steel structure after processing according to mode *I*, in addition to ferrite, there are regions of bainite with a granular morphology (Fig. 1, *b*), troostite (Fig. 1, *c*) and dispersed Fe_3C carbide particles (d_{Fe_3C} = 50 ÷ 250 nm) located within and at the boundaries of ferrite and bainite grains (Fig. 1, *c*). Coarser carbide particles up to 1 μm in size are also present. The average grain size of ferrite d_F decreased to 4.6 μm, while the average grain size of bainite (d_B) is 2.5 μm. The fraction of troostite segments decreased to 10.5 % and the interplanar distance in troostite is 0.17 μm (Fig. 1, *c*). The high dispersity of troostite is a result of accelerated cooling.

In the steel samples processed according to mode *II*, the structure consists of regions of ferrite, troostite, granulated and lath bainite, as well as the segments of the MA constituent and Fe_3C carbide particles (Fig. 1, *d* – *f*). The average size of ferrite grains decreased to 4.3 μm, and the sizes of the MA constituent ranges from 1 to 2 μm. The structure also contains coarse particles of Fe_3C carbide (up to 1 μm), although the fraction of finely dispersed carbides is lower compared to processing according to mode *I*. The fraction of troostite grains decreased to 7.5 %. In the case of processing according to mode *II*, the fraction of the bainite phase is higher.

The microhardness of the ferrite matrix increased to 205 HV_{50} after steel cooling according to mode *I* and to 225 HV_{50} after steel cooling according to mode *II*. Similarly, the microhardness of the bainite regions increased to 320 HV_{50} and 335 HV_{50}, respectively (refer to Table, where HV_F is the microhardness of ferrite; HV_B is the microhardness of bainite; $\sigma_{0.2}$ is the yield stress; σ_u is the ultimate tensile strength; ε is the plasticity; KCV is the impact toughness at various test temperatures).

The yield stress of the steel increased by 20 and 35 % after cross-helical rolling according to modes *I* and *II*, respectively. Additionally, the ultimate tensile strength increased by 20 and 75 % in the respective modes. However, there was only a slight decrease in plasticity. The higher level of strength properties observed after cooling according to mode *II* can be attributed to the formation of a higher fraction of the bainite phase, as well as the formation of lath bainite and segments of the MA phase.

During impact bending tests, it was observed that the steel samples in the hot rolled state exhibited higher fracture energy at ambient temperature (refer to Table; Fig. 2, *a*). However, as the test temperature decreased to –40 and –70 °C, the fracture toughness sharply decreased. All impact loading diagrams of the steel showed segments of sharp load decrease (indicated by arrow in Fig. 2, *a*). At negative test temperatures, a sharp decrease in the curves was observed immediately after reaching the maximum load. This form of load–deflection curves indicates the occurrence of avalanche crack propagations, which is characteristic of brittle fracture.

The fracture of the samples at low temperatures occurs through the mechanism of transcrystalline cleavage, as depicted in Fig. 3, *a* and *b*. Even at –40 °C, the fraction of brittle fracture is almost 100 %, as shown in Fig. 4, *a*.

In the temperature range of –40 ÷ –70 °C, the fracture surfaces exhibit a lack of tightening of the lateral faces and shear lips (represented as λ in Fig. 3, *d*), which are

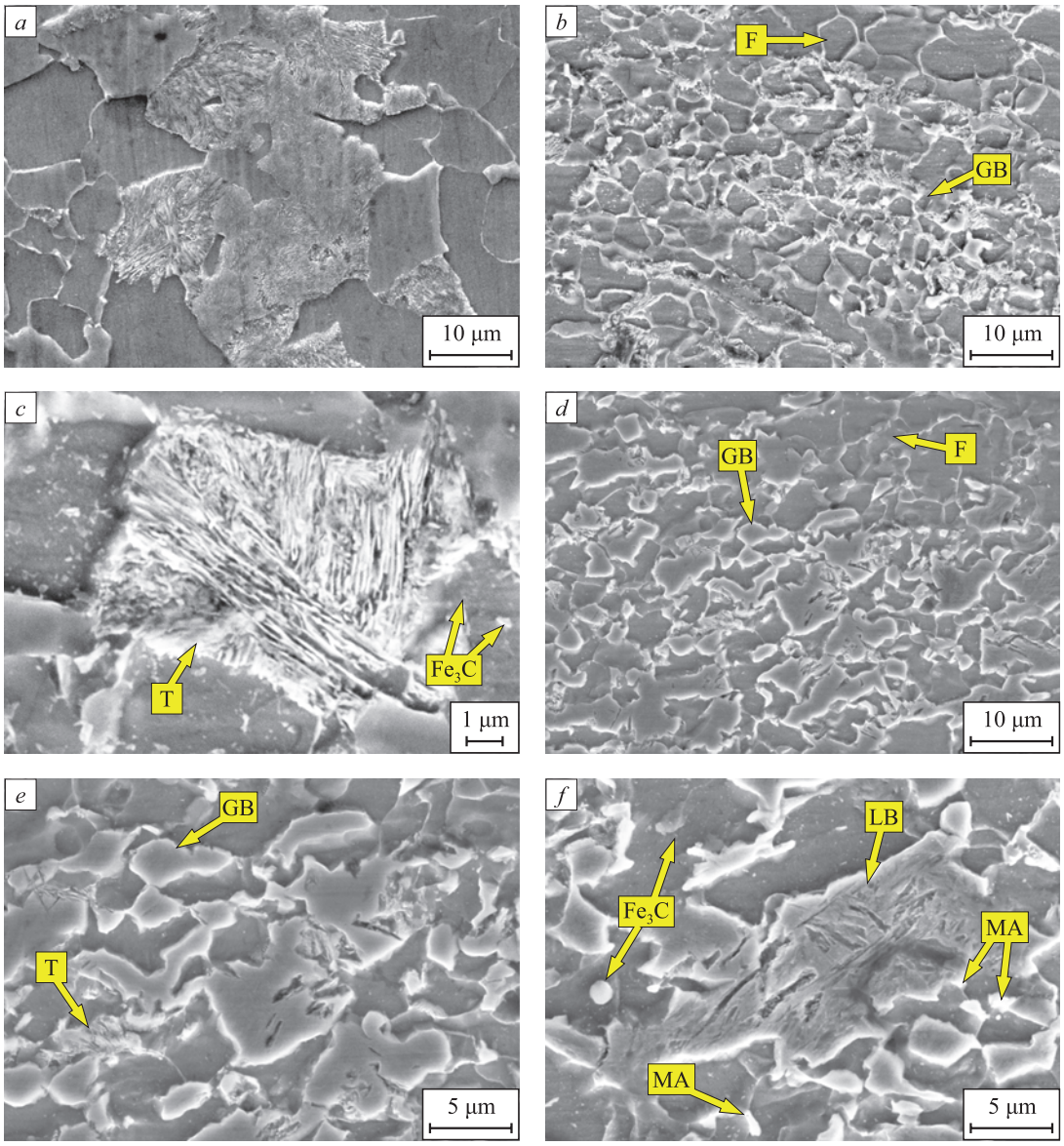

Fig. 1. SEM images of steel structures in hot-rolled state (*a*), after cross-helical rolling using mode *I* (*b*, *c*) and mode *II* (*d* – *f*)
(F – ferrite; GB – granular bainite; LB – lath bainite; T – troostite; MA – MA component)

Рис. 1. РЭМ-изображения структур стали в горячекатаном состоянии (*a*), после поперечно-винтовой прокатки по режимам *I* (*b*, *c*) и *II* (*d* – *f*)
(F – феррит; GB – гранулярный бейнит; LB – реечный бейнит; T – троостит; MA – MA составляющая)

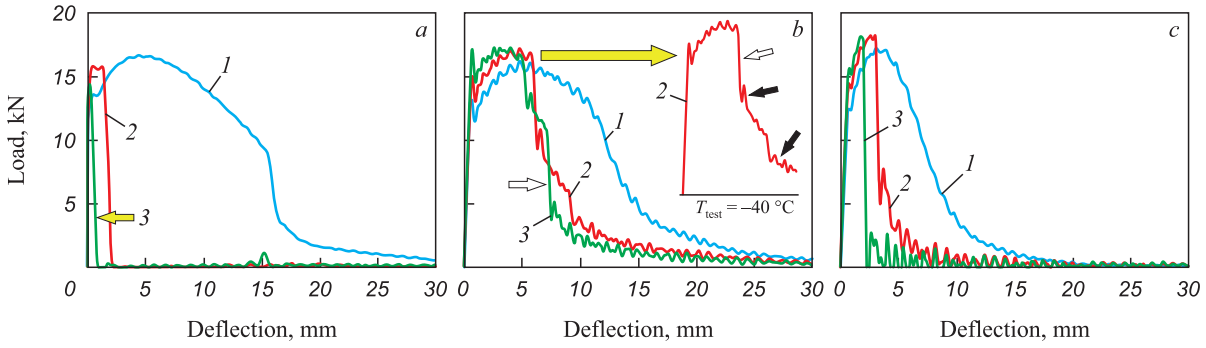

Fig. 2. Curves of impact loading of steel in the hot-rolled state (*a*), after treatments using mode *I* (*b*) and mode *II* (*c*):
1 – T_{test} = +20 °C; *2* – T_{test} = –40 °C; *3* – T_{test} = –70 °C

Рис. 2. Кривые ударного нагружения стали в горячекатаном состоянии (*a*), после обработок по режимам *I* (*b*) и *II* (*c*):
1 – T_{test} = +20 °C; *2* – T_{test} = –40 °C; *3* – T_{test} = –70 °C

Mechanical properties of X70 steel

Механические свойства стали категории прочности К60

State	HV_{50}	$\sigma_{0.2}$, MPa	σ_u, MPa	ε, %	KCV^{+20}, J/cm^2	KCV^{-40}, J/cm^2	KCV^{-70}, J/cm^2
Hot rolled	HV_F = 165	360	650	23.0	250	23	11
Processing according to mode *I*	HV_F = 205	440	760	20.5	245	185	160
	HV_B = 320						
Processing according to mode *II*	HV_F = 225	490	880	20.0	160	85	45
	HV_B = 335						

characteristic of macroplastic deformation (Fig. 3, *a*; Fig. 4, *b*). The temperature at which the steel undergoes a transition from a viscous to a brittle fracture mode, known as T_{50}, is –30 °C.

After cross-helical rolling of steel according to mode *I*, the fracture toughness of the samples at ambient temperature remains at a similar level to that of the hot rolled state (refer to Table). The loading diagram of these samples

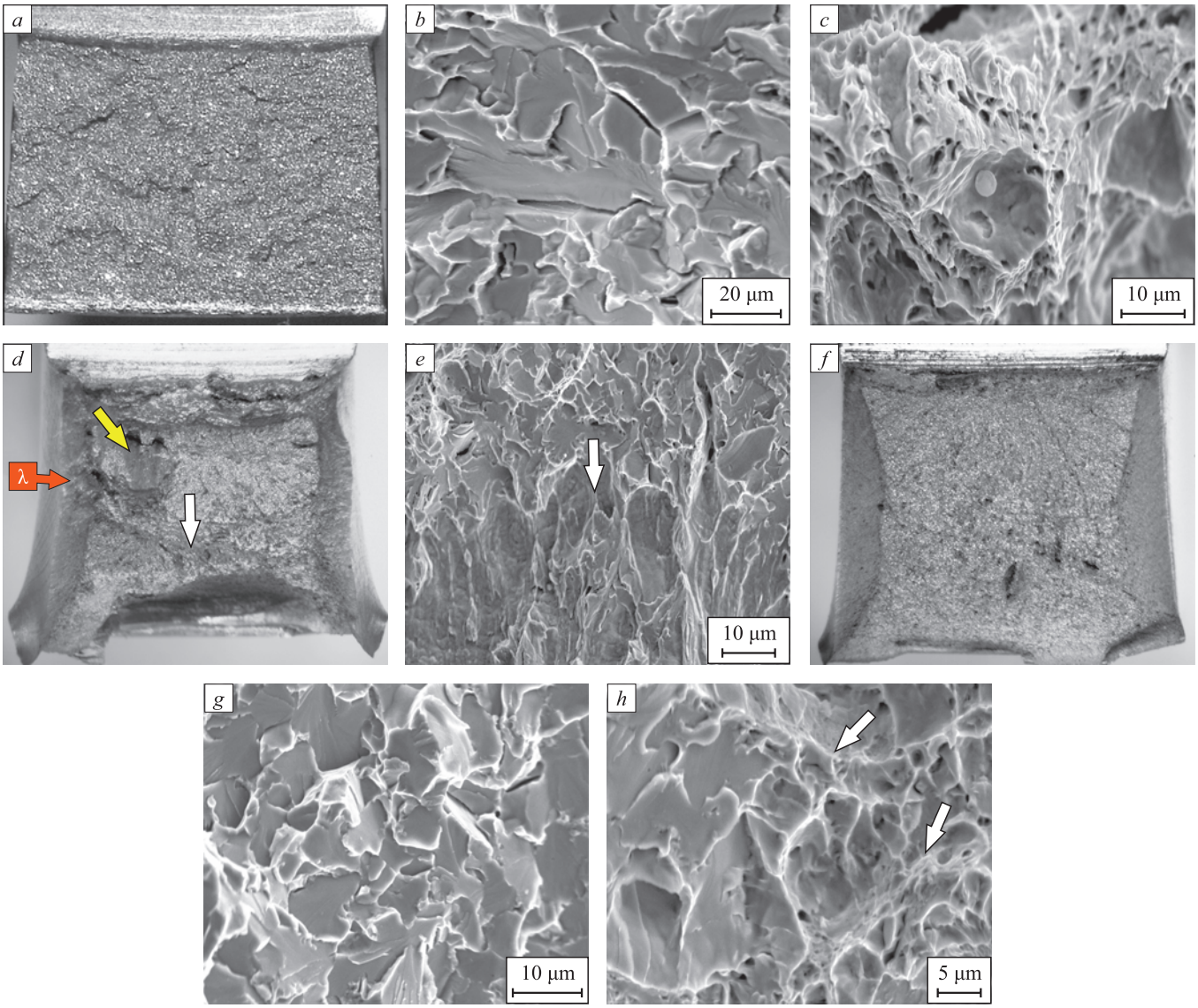

Fig. 3. Fracture surfaces of the impacted samples of steel in hot-rolled state at T_{test} = –40 °C (*a*, *b*), after treatment using mode *I* at T_{test} = +20 °C (*c*) and T_{test} = –40 °C (*d*, *e*) and using mode *II* at T_{test} = –40 °C (*f* – *h*)

Рис. 3. Поверхности разрушения ударных образцов стали в горячекатаном состоянии при T_{test} = –40 °C (*a*, *b*), после обработки по режиму *I* при T_{test} = +20 °C (*c*) и T_{test} = –40 °C (*d*, *e*) и по режиму *II* при T_{test} = –40 °C (*f* – *h*)

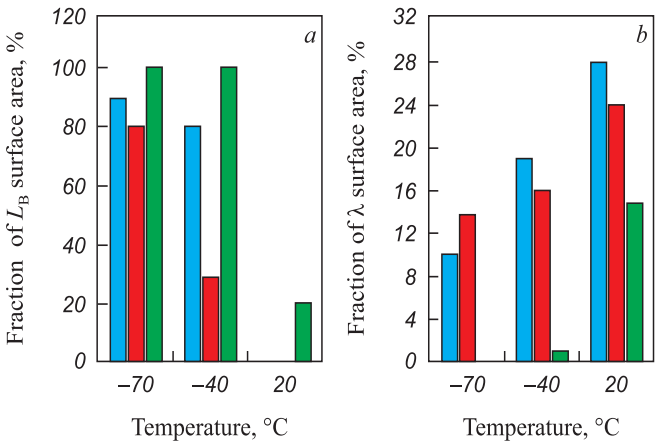

Fig. 4. Bar graphs of the area fractions of brittle fracture zones L_B (*a*) and shear lips (*b*) on steel fractures after hot rolling ( ) and after treatment using modes *I* and *II* (and)

Рис. 4. Гистограммы долей площади зон хрупкого разрушения L_B (*a*) и губ среза (*b*) на изломах стали после горячей прокатки ( ) и после обработки по режимам *I* и *II* (и)

does not exhibit linear segments of load drop (Fig. 2, *b*, curve *1*). Instead, oscillations of the load are detected, which are characteristic of high ductile steels and typical for fracture toughness analysis [13]. The nucleation and propagation of crack at all stages of fracture occur through the formation, growth and coalescence of pores (Fig. 3, *c*). Coarse carbide particles are present within the dimples observed on the fracture surface.

As the test temperature decreases, the fracture toughness, work of crack nucleation, and work of crack propagation in the steel processed according to mode I decrease (refer to Table and Fig. 2, *b*). However, these properties remain at a higher level compared to the hot rolled state. In the loading curves, segments of sharp load decrease were observed (Fig. 2, *b*; curves *2* and *3*, indicated by white arrow). However, after the avalanche propagation of the crack, there is a "blunting" of the crack. Further crack propagation is accompanied by plastic deformation (Fig. 2, *b*; black arrows). On the fracture surfaces of the destroyed samples, a clear transition from brittle to viscous fracture is observed (Fig. 3, *d*, *e*; indicated by white arrow). Additionally, the fracture surfaces exhibit segments of splitting (Fig. 3, *d*; indicated by yellow arrow), which contribute to an increase in fracture toughness by increasing the surface area upon crack formation [14]. Consequently, the energy required for crack development is higher, and the fraction of the brittle constituent in the fracture is lower (Fig. 4, *a*). At temperatures of –40 and –70 °C, the fraction of the brittle constituent in the fracture is 29 and 80 %, respectively. The presence of significant tightening on the lateral faces (Fig. 3, *d*), wide lips (Fig. 4, *b*), and rupture area (Fig. 3, *d*) down to –70 °C indicates a high degree of plastic deformation during crack propagation. This confirms higher resistance to fracture of the steel after processing according to mode *I*. The temperature of the viscous brittle transition, T_{50}, decreases to –55 °C.

In the case of continuous accelerated cooling after cross-helical rolling (mode *II*), the fracture toughness at ambient temperature is lower compared to all considered sates of the steel (refer to Table). At negative test temperatures, the work of crack nucleation and propagation is higher compared to the hot rolled state but lower than after processing according to mode *I* (Fig. 2, *c*). The sample exhibits a higher degree of macroplastic deformation compared to the hot rolled state, as evidenced by the presence of tightening on the lateral faces (Fig. 3, *f*) and shear lips (Fig. 4, *b*) even at temperatures as low as –70 °C. Oscillations are observed in the loading-deflection curves until reaching the maximum load. The highest load, at which the main crack begins to develop, is observed in the case of processing according to mode *II*. This results in the highest concentration of stresses near the crack tip. After reaching the maximum load, there is a sharp drop in the curve along a straight path. This stage corresponds to the brittle propagation of the crack through the mechanism of transcrystalline cleavage (Fig. 3, *g*). However, the fracture exhibits a mixed pattern, as it contains both cleavage facets and dimples on the fracture surface (Fig. 3, *h* – indicated by white arrows), indicating a certain degree of plastic deformation during the propagation of the main crack. The temperature of the viscous brittle transition, T_{50}, for the steel after processing according to mode *II* is –35 °C.

Discussion

The application of cross-helical rolling according to mode *I* offers a significant increase in the low temperature fracture toughness of X70 steel. This improvement is attributed to several factors, including the refinement of ferrite grain size (from 12 to 4.6 μm), a reduction in the size and fraction of the more brittle troostite phase, and a more homogeneous distribution of structural constituents (ferrite, troostite, bainite). These conclusions align with the experimental findings reported in references [3 – 6; 8]. During low temperature impact loading, there is an incompatibility of plastic deformation between the "soft" ferrite and the brittle troostite regions. The presence of larger troostite regions increases the likelihood of brittle cleavage crack development. By implementing accelerated cooling according to mode *I*, the formation of granular bainite occurs, and the structure releases finely dispersed carbides due to the holding at 530 °C. As a result, the fraction of troostite decreases to 10.5 %. Consequently, the propensity for brittle fracture during low temperature tests is reduced.

The absence of holding and continuous cooling in mode *II* restricts the release of carbides. As a result, the fraction of finely dispersed carbides in the ferrite matrix

after cooling according to mode *II* is lower compared to processing according to mode *I*. This leads to a higher carbon concentration in austenite and an increase in its stability [15]. Consequently, the subsequent decomposition of austenite occurs at lower temperatures, resulting in the formation of lath bainite and the presence of segments of the MA phase (Fig. 1, *f*). As a consequence, the fracture toughness of the steel after processing according to mode *II* is lower than after processing according to mode *I*. In the available literature [3; 16 – 19] focusing on the study of bainite structures, there is no consensus on which type of bainite phase provides higher fracture toughness for steel. Some studies have shown that the structure of acicular ferrite leads to higher fracture energies and a lower temperature of viscous brittle transition [16; 17]. On the other hand, the formation of granular bainite has been associated with lower fracture energies due to coarser grains and larger segments of the MA phase. However, other researchers [3; 18; 19] have mentioned that the structure of granular bainite offers higher fracture toughness compared to lath bainite and pearlite. These differing conclusions can be attributed to variations in carbon content and micro-dopants (such as niobium, vanadium, molybdenum, titanium, etc.) in the steels, as well as differences in the rolling temperature modes that influence the conditions of bainite phase formation. In the studied case with a carbon content of 0.13 wt. %, rolling in the ($\gamma + \alpha$) region results in significantly enriched overcooled austenite. Subsequent accelerated cooling leads to the formation of lath bainite and large segments of the MA constituent. This aligns with the higher strength observed in the bainite structure (335 HV_{50}). However, the more strained structure of lath bainite does not allow for sufficient fracture toughness to be achieved after processing according to mode *II*.

It is important to note that fracture toughness is not solely controlled by the properties of the more brittle phase, but also by the properties of the surrounding matrix [20]. Microregions with higher fracture toughness can inhibit the propagation of brittle fracture originating from adjacent regions with lower fracture toughness. This explains the higher low temperature fracture toughness observed in the steel with a dispersed structure after rolling according to mode *II*, in comparison to the hot rolled state. Additionally, the mixed viscous brittle pattern of fracture, with the presence of blunting of the brittle crack and alternating cleavage facets and dimple relief in the fractures (Fig. 3, *h*), further supports this observation.

Based on the experimental results, it can be assumed that for this specific X70 steel, the favorable type of bainite phase is granular rather than lath bainite. In order to achieve a higher increase in fracture toughness through accelerated cooling, it may be necessary to decrease the carbon content in the steel.

Conclusions

Cross-helical rolling combined with accelerated cooling and holding at 530 °C (mode *I*) enables the refinement of the granular structure of X70 steel from 12 to 4.6 μm. The resulting structure consists of ferrite, troostite, granular bainite and finely dispersed carbides Fe_3C. Continuous accelerated cooling after cross-helical rolling (mode *II*) leads to the presence of grains of ferrite, troostite, granular and lath bainite, as well as segments of the martensite-austenite phase and Fe_3C particles. Compared to the hot rolled state, both modes *I* and *II* result in a more homogeneous distribution of structural constituents (ferrite, troostite, bainite) and a lower fraction of troostite in the structure (10.5 and 7.5 %, respectively).

As a result of the refinement of the granular structure, formation of the bainite phase, and matrix hardening by carbides, the microhardness of the ferrite matrix in the steel increases to 205 and 225 HV_{50} in modes *I* and *II*, respectively, compared to the hot rolled state. In the bainite regions, the microhardness reaches 320 and 335 HV_{50}. The yield stress of the steel increases to 440 and 490 MPa, and the ultimate strength increases to 760 and 880 MPa in modes *I* and *II*, respectively.

After cross-helical rolling according to mode *I*, the fracture toughness at negative temperatures significantly increases ($KCV^{-70\,°C}$ = 160 J/cm^2) compared to the hot rolled state ($KCV^{-70\,°C}$ = 11 J/cm^2). The presence of significant tightening on the lateral faces and wide shear lips up to –70 °C indicates a high degree of plastic deformation during crack propagation. The temperature of the viscous brittle transition, T_{50}, decreased to –55 °C for the steel after rolling according to mode *I*.

References / Список литературы

1. Efron L.I. *Metal Science in "Big" Metallurgy. Pipe Steels*. Moscow: Metallurgizdat; 2012:696. (In Russ.).
Эфрон Л.И. *Металловедение в «большой» металлургии. Трубные стали*. Москва: Металлургиздат; 2012:696.
2. Ali M., Porter D., Kömi J., Eissa M., Faramawy H.E., Mattar T. Effect of cooling rate and composition on microstructure and mechanical properties of ultrahigh-strength steels. *Journal of Iron and Steel Research International*. 2019;26:1350–1365. https://doi.org/10.1007/s42243-019-00276-0
3. Jia T., Zhou Y., Jia X., Wang Z. Effects of microstructure on CVN impact toughness in thermomechanically processed high strength microalloyed steel. *Metallurgical and Materials Transactions A*. 2017;48:685–696. https://doi.org/10.1007/s11661-016-3893-9
4. Li X.C., Zhao J.X., Jia S.J., Lu G.Y., Misra R.D.K., Liu Q.Y., Li B. Ultrafine microstructure design of high strength pipeline steel for low temperature service: The significant impact on toughness. *Materials Letters*. 2021;303:130429. https://doi.org/10.1016/j.matlet.2021.130429
5. Derevyagina L.S., Gordienko A.I., Pochivalov Yu.I., Smirnova A.S. Modification of the structure of low-car-

bon pipe steel by helical rolling, and the increase in its strength and cold resistance. *Physics of Metal and Metallography*. 2018;119(1):83–91. https://doi.org/10.1134/S0031918X18010076

6. Surikova N.S., Vlasov I.V., Derevyagina L.S., Gordienko A.I., Narkevich N.A. Influence of cross-screw rolling modes on mechanical properties and fracture toughness of pipe steel. *Izvestiya. Ferrous Metallurgy*. 2021;64(1):28–37. (In Russ.). https://doi.org/10.17073/0368-0797-2021-1-28-37

   Сурикова Н.С., Власов И.В., Деревягина Л.С., Гордиенко А.И., Наркевич Н.А. Влияние режимов поперечно-винтовой прокатки на механические свойства и вязкость разрушения трубной стали. *Известия вузов. Черная металлургия*. 2021;64(1):28–37. https://doi.org/10.17073/0368-0797-2021-1-28-37
7. Huda N., Midawi A.R.H., Gianetto J., Lazor R., Gerlich A.P. Influence of martensite-austenite (MA) on impact toughness of X80 line pipe steels. *Materials Science and Engineering: A*. 2016;662:481–491. https://doi.org/10.1016/j.msea.2016.03.095
8. Kang N., Lee Y., Byun S., Kim K., Kim K., Chung J., Cho K. Quantitative analysis of microstructural and mechanical behavior for Fe–0.1C–(V, Nb) steels as a function of the final rolling temperature. *Materials Science and Engineering: A*. 2009;499(1-2):157–161. https://doi.org/10.1016/j.msea.2007.11.145
9. Rybin V.V., Malyshevskii V.A., Khlusova E.I. Structure and the properties of cold-resistant steels for the constructions of Northern design. *Voprosy materialovedeniya*. 2006;1(45):24–44. (In Russ.).

   Рыбин В.В., Малышевский В.А., Хлусова Е.И. Структура и свойства хладостойких сталей для конструкций северного исполнения. *Вопросы материаловедения*. 2006;1(45):24–44.
10. Hwang B., Lee C.G., Kim S.-J. Low-temperature toughening mechanism in thermomechanically processed high-strength low-alloy steels. *Metallurgical and Materials Transactions A*. 2011;42(3):717–728. https://doi.org/10.1007/s11661-010-0448-3
11. Derevyagina L.S., Gordienko A.I., Surikova N.S., Volochaev M.N. Effect of helical rolling on the bainitic microstructure and impact toughness of the low-carbon microalloyed steel. *Materials Science and Engineering: A*. 2021;816:141275. https://doi.org/10.1016/j.msea.2021.141275
12. Pallaspuro S., Kaijalainen A., Mehtonen S., Kömi J., Zhang Z., Porter D. Effect of microstructure on the impact toughness transition temperature of direct-quenched steels. *Materials Science and Engineering: A*. 2018;712:671–680. https://doi.org/10.1016/j.msea.2017.12.037
13. Khotinov V.A., Farber V.M., Morozova A.N. Evaluating the toughness of pipe steels by impact fracture curves. *Diagnostics, Resource and Mechanics of materials and structures*. 2015;(2):57–66. https://doi.org/10.17804/2410-9908.2015.2.057-066
14. Morozova A.N., Schapov G.V., Khotinov V.A., Farber V.M., Selivanova O.V. Influence of the direction of propagation of the main crack on the fracture mechanism upon impact bending of samples of high-viscous steel with a filamentary structure. Tensile Region. *Physics of Metals and Metallography*. 2019;120(9):919–924. https://doi.org/10.1134/S0031918X19070068
15. Wang J., Van Der Wolk P.J., Van Der Zwaag S. On the influence of alloying elements on the bainite reaction in low alloy steels during continuous cooling. *Journal of Materials Science*. 2000;35:4393–4404. https://doi.org/10.1023/A:1004865209116
16. Ghosh S., Mula S. Thermomechanical processing of low carbon Nb–Ti stabilized microalloyed steel: Microstructure and mechanical properties. *Materials Science and Engineering: A*. 2015;646:218–233. https://doi.org/10.1016/j.msea.2015.08.072
17. Lan H.F., Du L.X., Misra R.D.K. Effect of microstructural constituents on strength–toughness combination in a low carbon bainitic steel. *Materials Science and Engineering: A*. 2014;611:194–200. https://doi.org/10.1016/j.msea.2014.05.084
18. Hwang B., Lee C.G., Lee T.-H. Correlation of microstructure and mechanical properties of thermomechanically processed low-carbon steels containing boron and copper. *Metallurgical and Materials Transactions A*. 2010;41(1):85–96. https://doi.org/10.1007/s11661-009-0070-4
19. Jia S.-J., Li B., Liu Q.-Y., Ren Y., Zhang S., Gao H. Efects of continuous cooling rate on morphology of granular bainite in pipeline steels. *Journal of Iron and Steel Research International*. 2020;27(7):681–690. https://doi.org/10.1007/s42243-019-00346-3
20. Luo X., Chen X., Wang T., Pan S., Wang Z. Effect of morphologies of martensite–austenite constituents on impact toughness in intercritically reheated coarse-grained heat-affected zone of HSLA steel. *Materials Science and Engineering A*. 2018;710:192–199. http://dx.doi.org/10.1016/j.msea.2017.10.079

Information about the Authors / Сведения об авторах

Antonina I. Gordienko, *Cand. Sci. (Eng.), Research Associate of the Laboratory of Physical Mesomechanics and Non-Destructive Control Methods,* Institute of Strength Physics and Materials Science, Siberian Branch of Russian Academy of Sciences
ORCID: 0000-0002-4361-8906
E-mail: mirantil@ispms.ru

Il'a V. Vlasov, *Cand. Sci. (Eng.), Research Associate of the Laboratory of Physical Mesomechanics and Non-Destructive Control Methods,* Institute of Strength Physics and Materials Science, Siberian Branch of Russian Academy of Sciences
ORCID: 0000-0001-9110-8313
E-mail: viv@ispms.ru

Антонина Ильдаровна Гордиенко, *к.т.н., научный сотрудник лаборатории физической мезомеханики и неразрушающих методов контроля,* Институт физики прочности и материаловедения Сибирского отделения РАН
ORCID: 0000-0002-4361-8906
E-mail: mirantil@ispms.ru

Илья Викторович Власов, *к.т.н., научный сотрудник лаборатории физической мезомеханики и неразрушающих методов контроля,* Институт физики прочности и материаловедения Сибирского отделения РАН
ORCID: 0000-0001-9110-8313
E-mail: viv@ispms.ru

Yurii I. Pochivalov, *Cand. Sci. (Phys.-Math.), Leading Researcher of the Laboratory of Physical Mesomechanics and Non-Destructive Control Methods,* Institute of Strength Physics and Materials Science, Siberian Branch of Russian Academy of Sciences
ORCID: 0000-0003-0236-816X
E-mail: pochiv@ispms.ru

Юрий Иванович Почивалов, *к.ф.-м.н., ведущий научный сотрудник физической мезомеханики и неразрушающих методов контроля,* Институт физики прочности и материаловедения Сибирского отделения РАН
ORCID: 0000-0003-0236-816X
E-mail: pochiv@ispms.ru

Contribution of the Authors / Вклад авторов

A. I. Gordienko – formation of the basic concept, goals and objectives of research; writing the text; reviewing publications on the article topic; analysis of experimental data.

I. V. Vlasov – conducting experimental studies; processing results and data analysis; revision of the text.
Yu. I. Pochivalov – conducting experimental studies; processing results and data analysis.

А. И. Гордиенко – формирование основной концепции, цели и задач исследования; написание текста рукописи; литературный обзор публикаций по теме статьи; анализ экспериментальных данных.
И. В. Власов – проведение экспериментальных исследований; обработка результатов и анализ данных; доработка текста.
Ю. И. Почивалов – проведение экспериментальных исследований; обработка результатов и анализ данных.

Received 02.09.2022
Revised 16.11.2022
Accepted 29.11.2022

Поступила в редакцию 02.09.2022
После доработки 16.11.2022
Принята к публикации 29.11.2022